Original Article

# An analytic approach to the dosimetry of a new BEBIG $^{60}$Co high-dose-rate brachytherapy source

**Subhalaxmi Bhola, T. Palani Selvam, Sahoo Sridhar, Ramkrishna S. Vishwakarma**

Radiological Physics and Advisory Division, Bhabha Atomic Research Centre, Anushaktinagar, Mumbai, India

**Received on: 20.09.11** **Review completed on: 14.04.12** **Accepted on: 14.04.12**

## ABSTRACT

We present a simple analytic tool for calculating the dose rate distribution in water for a new BEBIG high-dose-rate (HDR) $^{60}$Co brachytherapy source. In the analytic tool, we consider the active source as a point located at the geometric center of the $^{60}$Co material. The influence of the activity distribution in the active volume of the source is taken into account separately by use of the line source-based geometric function. The exponential attenuation of primary $^{60}$Co photons by the source materials ($^{60}$Co and stainless-steel) is included in the model. The model utilizes the point-source-based function, f(r) that represents the combined effect of the exponential attenuation and scattered photons in water. We derived this function by using the published radial dose function for a point $^{60}$Co source in an unbounded water medium of radius 50 cm. The attenuation coefficients for $^{60}$Co and the stainless-steel encapsulation materials are deduced as best-fit parameters that minimize the different

**Key words:** Analytic method, brachytherapy, high-dose-rate, monte carlo, treatment planning

## Introduction

In clinical practice, high-dose-rate (HDR) $^{192}$Ir and $^{60}$Co brachytherapy sources are used. $^{192}$Ir sources are most commonly used, but the use of $^{60}$Co sources has increased because of its longer half-life (5.25 years) and its availability in miniaturized forms (with dimensions comparable to those of $^{192}$Ir HDR sources). The Ralstron remote after-loader which uses type 1, type 2 and type 3 $^{60}$Co HDR sources, was introduced for intracavitary treatments because of the longer half-life.[1] Presently, BEBIG HDR $^{60}$Co brachytherapy sources (old and new designs) are in widespread use for intra-cavitary treatments.[2,3] In a recently published study by Richter *et al*.,[4] the authors have compared the physical properties of $^{60}$Co and $^{192}$Ir HDR sources. They demonstrated that the integral dose due to radial dose fall-off is higher for $^{192}$Ir than for $^{60}$Co within the first 22 cm from the source. At larger distances, this relationship is reversed. Their study suggests that no advantage or disadvantage exists for $^{60}$Co sources compared with $^{192}$Ir sources with regard to clinical aspects. However, there are potential logistical advantages of $^{60}$Co sources because only 33% of the activity of $^{192}$Ir sources is needed to yield an equivalent dose-rate. Further, because of relatively long half life, $^{60}$Co sources can be used for much longer duration resulting in reduced operating costs.

The use of a brachytherapy source for clinical trials requires an extensive dosimetric data set either in the form of an American Association of Physicists in Medicine (AAPM) TG-43 parameters or in the form of a 2-D dose-rate lookup table.[5,6] According to AAPM TG-56, such data are needed for commissioning and verification purposes in radiotherapy treatment planning systems (RTPS).[7] The dosimetry data are usually generated by use of Monte Carlo methods. For example, Monte Carlo-based dosimetry data for HDR $^{60}$Co sources are reported in the literature.[1-3] and [8] An EGSnrc-based published study for new and old sources by Selvam and Bhola[8] demonstrated that the dose-rate data compare well with the GEANT4-based published data[2] and [3] for radial distances larger than 0.5 cm. Selvam and Bhola[8] have shown differences in dose values up to 9%

**Address for correspondence:**
Mrs. Subhalaxmi Bhola,
Radiological Physics and Advisory Division, Health, Safety and Environment Group, Bhabha Atomic Research Centre, Anushaktinagar, Mumbai - 400 094, India.
E-mail: subhalaxmi_bhola@yahoo.co.in

**Access this article online**

Quick Response Code:

Website: www.jmp.org.in

DOI: 10.4103/0971-6203.99228

for regions close to BEBIG $^{60}$Co sources when compared with GEANT4-based published work for these sources.[2] and [3] It was also demonstrated that the length of stainless-steel cable for the new BEBIG $^{60}$Co source considered by Granero *et al*.[3] in their GEANT simulations was 1 mm, although it was mentioned to be 5 mm.[8]

The Sievert integral algorithm is generally used in RTPS for dose calculation around brachytherapy sources.[9] For $^{125}$I, $^{169}$Yb, $^{137}$Cs and $^{192}$Ir brachytherapy sources, such analytic methods have already been established.[10-18] Our objective in the present study was to develop a simple analytic tool for calculating the 2D dose-rate distribution in water for the new model (Co0.A86) of a BEBIG $^{60}$Co HDR source. Using the analytic model, we calculated AAPM TG-43 dose parameters such as the dose-rate constant, radial dose function and anisotropy function for the above source in a 50-cm radius in an unbounded water medium. We also calculated the dose-rate look-up table in a Cartesian format. A comparison was made with previously published work.[8] The dose-rate data calculated with the use of the proposed analytic model could be used for verifying the results of treatment-planning systems or directly as input data for RTPS.

## Materials and Methods

### *New BEBIG $^{60}$Co source*

Analytic calculations were performed for the new model of the BEBIG $^{60}$Co HDR (model Co0.A86) brachytherapy source [Figure 1].[3] The new BEBIG $^{60}$Co HDR brachytherapy source[3] is very much similar, both in materials and design, to the old BEBIG $^{60}$Co HDR brachytherapy source (model GK60M21).[2] The new source design has a smaller active core of diameter 0.5 mm with a rounded capsule tip, whereas the old design has an active core of diameter 0.6 mm. The new source has a more rounded capsule tip. Both sources consist of a central cylindrical active core of length 3.5 mm, which is made of metallic $^{60}$Co. The active core is covered by a cylindrical stainless-steel capsule with an external diameter of 1 mm.

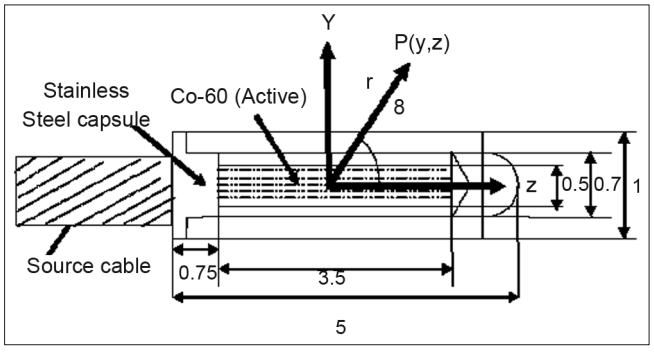


**Figure 1: Schematic diagrams of the new BEBIG $^{60}$Co high-dose-rate brachytherapy source (model Co0.A86), depicting geometric characteristics and materials. The coordinate axes used in this study are also shown with their origin situated in the geometric center of the active volume. All dimensions are in millimeters. Figures not drawn to scale**

### *TG-43 dose calculation formalism*

The TG43 report[5,6] has recommended the dose calculation algorithm for establishing the 2D dose-rate distribution in a water medium around cylindrically symmetric photon-emitting brachytherapy sources. The dose-rate at polar coordinates (r,θ) is written as

$$\dot{D}(r,\theta) = S_K \Lambda \frac{G_L(r,\theta)}{G_L(r_0,\theta_0)} g_L(r) F(r,\theta) \quad .....(1)$$

Here, the air-kerma strength, $S_k$, is defined as the product of the air-kerma rate $\dot{K}(r_c)$ measured at a calibration distance $r_c$ along the transverse bisector of the source in free space and the square of the distance $r_c$. $S_k$ has units of U (1U=1 μ*G*ym$^2$/h = 1 *c*Gycm$^2$/h).

$$S_K = \dot{K}(r_c) d^2 \quad .....(2)$$

The dose-rate constant, Λ, is defined as the dose-rate per $S_k$ along the transverse source bisector at the reference distance $r_0$ = 1 cm. The reference angle, $\theta_0$ defines the source transverse plane, and is specified to be 90$^0$ or π/2 radian. Λ has the units of cGy/h/U, which reduces to cm.

$$\Lambda = \dot{D}(r_0,\theta_0)/S_k . \quad .....(3)$$

The radial dose function, $g_L(r)$ , accounts for the effect of absorption and scatter in the medium along the transverse axis of the source, defined as follows:

$$g_L(r) = \dot{D}(r,\theta_0) G_L(r_0,\theta_0) / \dot{D}(r_0,\theta_0) G_L(r,\theta_0) \quad .....(4)$$

The anisotropy function, $F(r, \theta)$, accounts for anisotropy of the dose distribution around the source, and is defined as follows:

$$F(r,\theta) = \dot{D}(r,\theta) G_L(r,\theta) / s\dot{D}(r,\theta) G_L(r,\theta) . \quad .....(5)$$

The geometry function, $G_L(r,\theta)$ , accounts for the spatial distribution of radioactivity within the source, and is defined as follows:

point source approximation, $G_L(r,\theta) = 1/r^2$, .....(6.a)

line-source approximation, $G_L(r,\theta) = \frac{\beta}{Lr\sin\theta}$ , .....(6.b)

where β (in radians) is the angle subtended by the source to the point of interest, $(r, \theta)$.[5,6]

### *Analytic approach*

#### *Monoenergetic point photon source in water*

The absorbed dose-rate in water at a distance r (cm) away from a point isotropic monoenergetic photon source is given by,

$$\dot{D}(r) = A k \frac{1}{4\pi r^2} E\left[\mu_{en}(E)/\rho\right]_{wat} e^{-\mu_w r} B \quad .....(7)$$

where A denotes the activity of the source (in Bq), E is the energy emitted by the source (in MeV) per photon, k is the constant converting the unit MeV/gm to Gy, $\left[\mu_{en}(E)/\rho\right]_{air}^{wat}$ the mass energy absorption coefficient of water in units

of cm$^2$/gm for photon of energy E, and B is the energy-absorption build-up factor.[19] B is defined as the absorbed dose-rate from both the primary and the scattered photons in an infinite water medium divided by the absorbed dose-rate from only primary photons. The assumption made in equation 7 is that the energy lost by photons in the scattering and absorption events is absorbed locally in the medium. This means that the range of secondary electrons (photo electrons, compton electrons and delta-rays) is assumed to be negligible. In the energy range relevant to brachytherapy sources, this assumption has little impact on the calculated dose-rate.

$S_k$ at a distance r away from a point monoenergetic photon source of energy E and activity A can be obtained analytically:

$$S_k = A\frac{1}{4\pi}Ek\left[\mu_{en}(E)/r\right]_{air} \quad , \qquad .....(8)$$

where $\left[\mu_{en}(E)/r\right]_{air}$ is the mass–energy absorption coefficient of air for the energy E. It should be noted that $S_k$ is expressed in terms of the recommended unit U (= 1 cGycm$^2$/h).

The dose-rate $\dot{D}(r)$ in water per $S_k$ due to a point monoenergetic point photon source of energy E is then given by

$$\frac{D(r)}{S_k} = \left[\mu_{en}(E)/r\right]_{air}^{wat} f(r)\frac{1}{r^2} \qquad .....(9)$$

where $f(r) = Be^{-\mu w r}$, $\left[\mu_{en}(E)/r\right]_{air}^{wat}$ is the ratio of the mass–energy absorption coefficient of water to air at photon energy E, which is equal to 1.112 at $^{60}$Co energies.[20] The value of $\left[\mu_{en}(E)/r\right]_{air}^{wat}$ is constant (=1.112) in the photon energy range between 0.15 MeV and 3 MeV.[20] As compton scattering is the predominant process in water at $^{60}$Co energies, one can write $\left[\mu_{en}(E)/r\right]_{air}^{wat} = \left[\frac{\langle Z/A\rangle}{\langle Z/A\rangle}\right]_{air}^{wat} = 1.112$, where $\left[\frac{\langle Z/A\rangle}{\langle Z/A\rangle}\right]_{air}^{wat}$ is the ratio of electrons/g between water and air. The values of $\langle Z/A\rangle$ for water and air are 0.555 and 0.499, respectively.[20]

The functional form of f(r) for $^{60}$Co brachytherapy sources has been presented by many authors. Kartha *et al.*[21] have given an analytical expression, $f(r) = \exp\{[0.73/E^{0.05}s]-1\}\mu r$, where E is the photon energy (for $^{60}$Co, it is 1.25 MeV), μ is the linear attenuation coefficient in water and r is the distance from the source. Meisberger[22] approximated *f(r)* by the ratio of the air kerma in water to air kerma in air. He fitted the *f(r)* data to a third-order polynomial function, $f(r) = A + Br + Cr^2 + Dr^3$ (valid up to 10 cm from the source), with coefficients A = 0.99423, B = -5.318x10$^{-3}$/ cm, C=- 2.610x10$^{-3}$/cm$^2$ and D = 13.27 x 10$^{-5}$/cm$^3$. Van Kleffens and Starr[23] provided an expression, $f(r) = (1+ ar^2) / (1+br^2)$, with a= 10x10$^{-3}$/cm$^2$ and b=14.50x10$^{-3}$/cm$^2$. Kornelson and Young[24] have given a functional form for the build-up factor, $B(r) = 1 + k_a(\mu r)^{k_b}$ where μ is the linear attenuation coefficient at $^{60}$Co energies, $k_a$ = 0.896 and $k_b$ = 1.063. Angelopoulos *et al.*[25] have provided data for f(r) for distances r = 1–9 cm in a 10-cm-radius water phantom. The most recent published study for a point $^{60}$Co source in water gives a radial dose function, $g_p(r)$, in an unbounded water medium by Papagiannis *et al.*[1]

$$g_p(r) = -1.418\times10^{-4}r^2 - 1.470\times10^{-2}rs + 1.015 \qquad .....(10)$$

Note that equation 10 is based on water-kerma as it was verified in a previously published work.[8] From equation 10, $f(r)$ can be derived as follows:

According to the TG-43 protocol,[5,6]

$$g_p(r) = \frac{\dot{D}(r)r^2}{\dot{D}(r_0 \to r_0^2} \qquad .....(11)$$

where $r_0$ = 1 cm.

By using equation 7 in 11, one obtains

$$g_p(r) = \frac{Be^{-\mu_w r}}{Be^{-\mu_w r_0}} = \frac{f(r)}{f(r_o)} \qquad .....(12)$$

$$f(r) = f(r_0)g_p(r) \qquad .....(13)$$

Here, $f(r_o)$ = 0.9864 is calculated at $r_0$ = 1 cm with the use of Mesiberger's polynomial[22] for *f(r)*. In our analytical model, we make use of equation 13.

### *Monoenergetic bare cylindrical source in water*

The dose-rate $\dot{D}(r,\theta)$ at a point *(r, θ)* in water per $S_k$ for a bare cylindrical source of photon energy, E, can be written as

$$\frac{\dot{D}(r,\theta)}{S_k} = \left[\mu_{en}/r\right]_{air}^{wat}\frac{1}{N}\sum_{i=1}^{N} f(r_i)\frac{1}{r_i^2} \qquad .....(14)$$

In the above formalism, the active cylindrical source is divided into N active segments, and each segment is treated as a point source and $r_i$ is the distance between the $i^{th}$ source element to the point (r, θ). The above equation is further simplified as follows:

$$\frac{\dot{D}(r,\theta)}{S_k} = [\mu_{en}/r]_{air}^{wat} f(r)G_L(r,\theta) \qquad .....(15)$$

where, *r* is the distance between the center of the active length and the point of interest (r, θ). In equation 15, an assumption is made that the entire activity is concentrated at the geometric center of the cylinder. The influence of the activity distribution in the cylindrical volume is taken into account separately by use of the line-source-based geometry function, $G_L(r,\theta)$. A simple calculation for a cylindrical bare active $^{60}$Co source of 3.5 mm length and

0.5 mm diameter (these are typical active dimensions of the new BEBIG $^{60}$Co source) by using equations 14 and 15 give a dose-rate value of 4.23 cGy/h/U at 5 mm along the transverse axis of the source. This suggests that equation 15 can be used for dose calculations.

Papagiannis *et al.*[26] observed that close to $^{192}$Ir HDR sources, it is the inherent influence of the "exact" geometry function[5,18,27] that determines the dose-rate distribution. In order to verify that the use of $G_L(r,\theta)$ in equation (15) produces reasonably accurate results, we calculated an "exact" geometry function, $G_{ex}(r,\theta)$, by using the Monte Carlo integration approach as adapted by Karaiskos *et al.*[18],

$$G_{ex}(r,\theta)=\frac{1}{N}\sum_{i=1}^{N}\frac{1}{|r'-r|^2}=\frac{1}{N}\sum_{i=1}^{N}=\frac{1}{r_i^2} \qquad .....(16)$$

where $r_i^2=|r'-r|^2$, with $r_i$ being the distance between the i$^{th}$ Monte Carlo generated point and the calculation point $(r, \theta)$. The Monte Carlo values of $G_{ex}(r,\theta)$ at distances 1, 2 and 5 mm from the source center along the transverse axis $(\theta=90^0)$ are larger only by 1.23%, 0.5% and 0.1%, respectively, when compared with the corresponding values of $G_L(r,\theta)$.

### *Real cylindrical source in water*

Cassell proposed the quantization method (decomposition of the source into small cells) for brachytherapy dose calculations.[28] This algorithm is similar to the Sievert integral model described by Williamson.[10] According to Cassell,[28] the dose-rate $\dot{D}$ (r, θ) in water at a point P(r, θ), in units of cGy/h can be obtained from the following equation:

$$\dot{D}(r,\theta)=\dot{K}_R\left[\mu_{en}/\rho\right]_{air}^{wat}e^{\mu_s t_1+\mu_f t_2}\frac{1}{N}\left[\sum_{j=1}^{N}\exp(-\mu_s r_{s_j}-\mu_f r_{f_j})\frac{f(r_{w_j})}{r_j^2}\right] \qquad .....(17)$$

Note that the reference air-kerma rate, $\dot{K}_R$, is equivalent to $S_k$ of the source.[6]

In the quantization method, the active part of the cylindrical source is divided into N source elements, which are treated as point sources. For each elemental source, the dose-rate is calculated by multiplying $\left[\mu_{en}/\rho\right]_{air}^{wat}$ and correcting for the inverse square of the distance, tissue attenuation, self-absorption and filter attenuation by use of an exponential correction over the line between the elemental source and the calculation point. Symbols in equation 17 have the following meaning: $\mu_s$, $\mu_f$ and $\mu_w$ are the linear attenuation coefficient of the active source, of the filtration material and of water, respectively. $t_1$ and $t_2$ are the active radii of the source and the encapsulation thickness, respectively. $r_{s_j}$, $r_{f_j}$ and $r_{w_j}$ are the distances traveled by photons within the source core, filter material and the water medium, respectively, and $r_j$ is the distance between the center of the source and the calculation point P(r, θ). Photon paths in different media are depicted in [Figure 2].

$$r_j=r_{s_j}+r_{f_j}+r_{w_j} \qquad .....(18)$$

Motivated by our analytic model described for a bare cylindrical source, we consider that the total activity is concentrated at the center of the $^{60}$Co material instead of being distributed throughout its volume. The influence of the distribution of activity in the source on the dose-rate is taken into account separately by the line-source-based geometry function $G_L(r,\theta)$. According to our simplified model, the dose-rate $\dot{D}$ (r, θ) per $S_k$ at a point $(r, \theta)$ can be written as follows:

$$\frac{\dot{D}(r,\theta)}{S_k}=\left[\frac{\mu_{en}}{\rho}\right]_{air}^{wat}e^{(\mu_s t_1+\mu_f t_2)}e^{(-\mu_s r_s-\mu_f r_f)}f(r_w)G_L(r,\theta) \qquad .....(19)$$

where $r_s$, $r_f$ and $r_w$ (= r - $r_s$ – $r_f$) are the distances traveled by photons within the source core, filter material and water, respectively, as is shown in [Figure 2]. In the calculations, the function f(r) (equation 13) is evaluated at $r_w$. When θ = $\theta_0$, $r_s = t_1$, $r_f = t_2$. For the new design of the $^{60}$Co source, $t_1$ = 0.025 mm, $t_2$ = 0.015 cm and $t_1 + t_2$ = 0.04 cm. Therefore, $r_w$ = r and $f(r_w)$ = f(r) for values of r larger than 2.5 mm. For θ = $\theta_0$, equation 19 can be written as:

$$\frac{\dot{D}(r,\theta_0)}{S_k}=\left[\frac{\mu_{en}}{\rho}\right]_{air}^{wat}f(r)G_L(r,\theta_0) \qquad .....(20)$$

Equation 20 is same as equation 15 when we set θ = $\theta_0$ in equation 15. For the calculation of the transverse axis dose-rate distribution, equation 20 is good enough. When we set r = $r_0$ = 1 cm in equation 20,

$$\frac{\dot{D}(r_0,\theta_0)}{S_k}=\Lambda=\left[\frac{\mu_{en}}{\rho}\right]_{air}^{wat}f(r_0)G_L(r_0,\theta) \qquad .....(21)$$

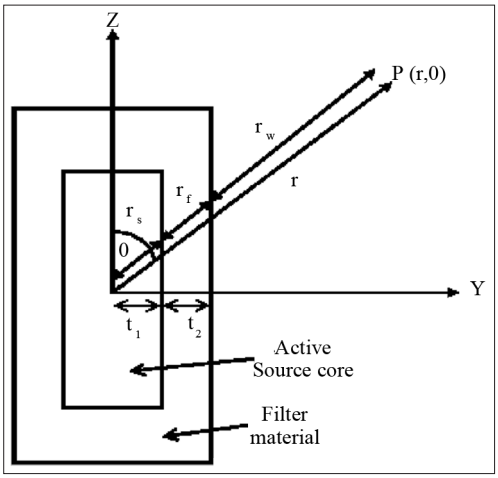


**Figure 2: Simplified geometry used in the present analytical model. A point $^{60}$Co source is positioned at the geometric center of the inactive metallic $^{60}$Co material**

Equation 21 is a general expression for the dose-rate constant of a monoenergetic photon source of active length L.

### *Dose-rate calculation for BEBIG source by use of the analytic tool*

We have adapted the analytical tool described above for calculating dose-rate distributions in water around the new BEBIG $^{60}$Co HDR source. We used equation 19 for this purpose. The lengths of stainless steel cable considered in the analytical calculations are 1 mm and 5 mm. Dose-rate calculations are carried out as functions of polar coordinates (r, θ) and Cartesian coordinates (y,z). In the calculations, the radial distance r is varied from 1 mm to 14 cm (in 2.5- mm intervals up to 3 cm and 1-cm intervals from 3 cm to 14 cm), and the polar angle θ is varied from 0° to 179° (in 2° intervals) for each r, with the 180° angle referring to the source cable side.

The analytically calculated dose-rate values for the new BEBIG $^{60}$Co source with 1 mm and 5 mm cable lengths by use of equation 19 compare well with the published values for regions other than those close to the source axis.[3,8] For example, for the regions close to the source axis, the analytically calculated dose-rates are higher by up to 10% when compared with the published Monte Carlo-based values.[3,8] In order to verify whether this disagreement is due to simplifications made in the analytic model, we carried out a test calculation by using equation 17. Yet, the same disagreement was observed. For the analytical calculations, we used $\mu_s$ = 0.47/cm, $\mu_f$ = 0.43/cm and $\mu_w$ = 0.063/cm, all obtained at $^{60}$Co energies.[13]

Most of the currently available RTPS make use of the Sievert algorithm[9] to generate dose distributions for filtered line sources. Frequently, the RTPS, based on this algorithm, does not produce accurate calculations[5] for the regions close to the source axis. TG-43[5] recommends treating the attenuation coefficients as parameters of the best fit for minimizing the deviations between the Sievert model predictions and the other calculated results. Self-absorption by the source core ($\mu_s$) and attenuation by the filtration material ($\mu_f$) to be used in such algorithms are generally derived by comparing the dose results with the Monte Carlo results. For example, Ballester *et al*.[13] and Casal *et al*.[14] adapted this approach in their Sievert integral-based $^{137}$Cs dosimetry and derived best-fit parameters for $\mu_s$ and $\mu_f$. Similarly, Pérez Calatayud *et al*.[16] derived best-fit parameters for $\mu_s$ and $\mu_f$ in their quantization method-based dosimetry study on CDC-type miniaturized $^{137}$Cs sources[15] and the best-fit parameter for μ for $^{192}$Ir wires.

Guided by the above-mentioned published work, we treated the parameters $\mu_s$ and $\mu_f$ as free-fit parameters. Instead of using the actual values of $\mu_s$ (= 0.47/cm) and $\mu_f$ (= 0.43/cm) at $^{60}$Co energies,[13] we used the fitted values $\mu_s$ = 0.25/cm and $\mu_f$ = 0.25/cm for the new BEBIG $^{60}$Co HDR source [Table 1]. For the above-described analytic method, computer software has been developed in $C_{++}$ computer-programming language. The software generates a complete dosimetry dataset around the source. The data include TG-43 parameters and a 2D look-up table. For the calculation of $g_L(r)$ and $F(r,\theta)$, we used $G_L(r,\theta)$. This is consistent with the updated TG-43 formalism.[6]

**Table 1: Actual and fitted values of linear attenuation coefficients for source and filtration materials $\mu_s$ and $\mu_f$, respectively, for the new BEBIG $^{60}$Co source**

| *Linear attenuation coefficient* | $\mu_s$ *(/cm)* | $\mu_f$ *(/cm)* |
|---|---|---|
| Actual value | 0.47 | 0.43 |
| Fitted value | 0.25 | 0.25 |

**Table 2: Comparison of dose rate constants of old and new BEBIG $^{60}$Co sources**

| *Source model* | *This work* | *Published work* | |
|---|---|---|---|
| Model GK60M21 (old) | 1.088 | 1.087[a] | 1.093 ± 0.002[c] |
| Model Co0.A86 (new) | 1.088 | 1.084[b] | 1.097 ± 0.002[c] |

[a]Ref 2 , [b]Ref 3, [c]Ref 8

**Table 3: Comparison of analytically calculated (this work) and Monte Carlo-based published data of radial dose function, $g_L(r)$, of the new BEBIG $^{60}$Co HDR source**

| *Radial distance (cm)* | *This work* | *Published (Ref 8)* |
|---|---|---|
| 0.1 | 0.904 | 0.830 |
| 0.15 | 1.023 | 0.961 |
| 0.2 | 1.022 | 1.037 |
| 0.25 | 1.022 | 1.072 |
| 0.3 | 1.021 | 1.077 |
| 0.35 | 1.020 | 1.066 |
| 0.4 | 1.019 | 1.050 |
| 0.45 | 1.018 | 1.037 |
| 0.5 | 1.018 | 1.028 |
| 0.6 | 1.016 | 1.019 |
| 0.75 | 1.014 | 1.011 |
| 1 | 1.000 | 1.000 |
| 1.5 | 1.002 | 0.991 |
| 2 | 0.994 | 0.983 |
| 2.5 | 0.987 | 0.974 |
| 3 | 0.979 | 0.967 |
| 4 | 0.962 | 0.95 |
| 5 | 0.952 | 0.938 |
| 6 | 0.930 | 0.916 |
| 7 | 0.914 | 0.9 |
| 8 | 0.899 | 0.884 |
| 10 | 0.863 | 0.849 |
| 12 | 0.832 | 0.81 |
| 15 | 0.779 | 0.759 |
| 20 | 0.676 | 0.664 |

**Table 4: Anisotropy function F(r,θ) values for the new (model Co0.A86) BEBIG $^{60}$Co HDR source.**

| | Radial distance r (cm) | | | | | | | | | | | | | | | |
|---|---|---|---|---|---|---|---|---|---|---|---|---|---|---|---|---|
| θ *(deg)* | *0.25* | *0.5* | *0.75* | *1* | *1.5* | *2* | *3* | *4* | *5* | *6* | *7* | *8* | *10* | *12* | *15* | *20* |
| 0 | | 0.953 | 0.953 | 0.953 | 0.953 | 0.953 | 0.953 | 0.953 | 0.954 | 0.954 | 0.954 | 0.954 | 0.954 | 0.955 | 0.955 | 0.956 |
| 1 | | 0.953 | 0.953 | 0.953 | 0.953 | 0.953 | 0.953 | 0.953 | 0.954 | 0.954 | 0.954 | 0.954 | 0.954 | 0.955 | 0.955 | 0.956 |
| 2 | | 0.953 | 0.953 | 0.953 | 0.953 | 0.953 | 0.953 | 0.953 | 0.954 | 0.954 | 0.954 | 0.954 | 0.954 | 0.954 | 0.955 | 0.956 |
| 3 | | 0.953 | 0.953 | 0.953 | 0.953 | 0.953 | 0.953 | 0.953 | 0.953 | 0.954 | 0.954 | 0.954 | 0.954 | 0.954 | 0.955 | 0.956 |
| 4 | | 0.953 | 0.953 | 0.953 | 0.953 | 0.953 | 0.953 | 0.953 | 0.953 | 0.954 | 0.954 | 0.954 | 0.954 | 0.954 | 0.955 | 0.956 |
| 5 | | 0.953 | 0.953 | 0.953 | 0.953 | 0.953 | 0.953 | 0.953 | 0.953 | 0.953 | 0.954 | 0.954 | 0.954 | 0.954 | 0.955 | 0.955 |
| 6 | | 0.953 | 0.953 | 0.953 | 0.953 | 0.953 | 0.953 | 0.953 | 0.953 | 0.953 | 0.953 | 0.954 | 0.954 | 0.954 | 0.955 | 0.955 |
| 8 | | 0.953 | 0.953 | 0.953 | 0.953 | 0.953 | 0.953 | 0.953 | 0.953 | 0.953 | 0.953 | 0.953 | 0.954 | 0.954 | 0.954 | 0.955 |
| 10 | | 0.966 | 0.966 | 0.966 | 0.966 | 0.966 | 0.966 | 0.966 | 0.966 | 0.966 | 0.966 | 0.967 | 0.967 | 0.967 | 0.968 | 0.968 |
| 15 | | 0.975 | 0.975 | 0.975 | 0.975 | 0.975 | 0.975 | 0.975 | 0.975 | 0.975 | 0.975 | 0.975 | 0.975 | 0.976 | 0.976 | 0.976 |
| 20 | | 0.983 | 0.983 | 0.983 | 0.983 | 0.983 | 0.983 | 0.983 | 0.983 | 0.983 | 0.983 | 0.983 | 0.983 | 0.984 | 0.984 | 0.984 |
| 25 | | 0.988 | 0.988 | 0.988 | 0.988 | 0.988 | 0.988 | 0.988 | 0.988 | 0.988 | 0.988 | 0.988 | 0.988 | 0.988 | 0.988 | 0.989 |
| 30 | | 0.991 | 0.991 | 0.991 | 0.991 | 0.991 | 0.991 | 0.991 | 0.991 | 0.991 | 0.991 | 0.991 | 0.991 | 0.991 | 0.992 | 0.992 |
| 40 | | 0.995 | 0.995 | 0.995 | 0.995 | 0.995 | 0.995 | 0.995 | 0.995 | 0.995 | 0.995 | 0.995 | 0.995 | 0.995 | 0.995 | 0.995 |
| 50 | | 0.997 | 0.997 | 0.997 | 0.997 | 0.997 | 0.997 | 0.997 | 0.997 | 0.997 | 0.997 | 0.997 | 0.997 | 0.997 | 0.997 | 0.998 |
| 60 | 0.999 | 0.999 | 0.999 | 0.999 | 0.999 | 0.999 | 0.999 | 0.999 | 0.999 | 0.999 | 0.999 | 0.999 | 0.999 | 0.999 | 0.999 | 0.999 |
| 70 | 0.999 | 0.999 | 0.999 | 0.999 | 0.999 | 0.999 | 0.999 | 0.999 | 0.999 | 0.999 | 0.999 | 0.999 | 0.999 | 0.999 | 1.000 | 1.000 |
| 80 | 1.000 | 1.000 | 1.000 | 1.000 | 1.000 | 1.000 | 1.000 | 1.000 | 1.000 | 1.000 | 1.000 | 1.000 | 1.000 | 1.000 | 1.000 | 1.000 |
| 90 | 1.000 | 1.000 | 1.000 | 1.000 | 1.000 | 1.000 | 1.000 | 1.000 | 1.000 | 1.000 | 1.000 | 1.000 | 1.000 | 1.000 | 1.000 | 1.000 |
| 100 | 1.000 | 1.000 | 1.000 | 1.000 | 1.000 | 1.000 | 1.000 | 1.000 | 1.000 | 1.000 | 1.000 | 1.000 | 1.000 | 1.000 | 1.000 | 1.000 |
| 110 | 0.999 | 0.999 | 0.999 | 0.999 | 0.999 | 0.999 | 0.999 | 0.999 | 0.999 | 0.999 | 0.999 | 0.999 | 0.999 | 0.999 | 1.000 | 1.000 |
| 120 | 0.999 | 0.999 | 0.999 | 0.999 | 0.999 | 0.999 | 0.999 | 0.999 | 0.999 | 0.999 | 0.999 | 0.999 | 0.999 | 0.999 | 0.999 | 0.999 |
| 130 | | 0.997 | 0.997 | 0.997 | 0.997 | 0.997 | 0.997 | 0.997 | 0.997 | 0.997 | 0.997 | 0.997 | 0.997 | 0.997 | 0.997 | 0.998 |
| 140 | | 0.995 | 0.995 | 0.995 | 0.995 | 0.995 | 0.995 | 0.995 | 0.995 | 0.995 | 0.995 | 0.995 | 0.995 | 0.995 | 0.995 | 0.995 |
| 150 | | 0.991 | 0.991 | 0.991 | 0.991 | 0.991 | 0.991 | 0.991 | 0.991 | 0.991 | 0.991 | 0.991 | 0.991 | 0.991 | 0.992 | 0.992 |
| 155 | | | 0.987 | 0.988 | 0.988 | 0.988 | 0.988 | 0.988 | 0.988 | 0.988 | 0.988 | 0.988 | 0.988 | 0.988 | 0.988 | 0.989 |
| 160 | | | 0.983 | 0.983 | 0.983 | 0.983 | 0.983 | 0.983 | 0.983 | 0.983 | 0.983 | 0.983 | 0.983 | 0.984 | 0.984 | 0.984 |
| 165 | | | – | 0.975 | 0.975 | 0.975 | 0.975 | 0.975 | 0.975 | 0.975 | 0.975 | 0.975 | 0.975 | 0.976 | 0.976 | 0.976 |
| 170 | | | – | 0.958 | 0.958 | 0.958 | 0.958 | 0.958 | 0.959 | 0.959 | 0.959 | 0.959 | 0.959 | 0.960 | 0.960 | 0.961 |
| 172 | | – | – | 0.930 | 0.930 | 0.930 | 0.931 | 0.931 | 0.931 | 0.931 | 0.931 | 0.931 | 0.932 | 0.932 | 0.933 | 0.934 |
| 174 | | – | – | 0.931 | 0.931 | 0.931 | 0.931 | 0.931 | 0.931 | 0.931 | 0.932 | 0.932 | 0.932 | 0.933 | 0.933 | 0.934 |
| 175 | | – | – | 0.931 | 0.931 | 0.931 | 0.931 | 0.931 | 0.931 | 0.931 | 0.932 | 0.932 | 0.932 | 0.933 | 0.933 | 0.934 |
| 176 | | – | – | 0.931 | 0.931 | 0.931 | 0.931 | 0.931 | 0.931 | 0.932 | 0.932 | 0.932 | 0.932 | 0.933 | 0.933 | 0.935 |
| 177 | | – | – | 0.931 | 0.931 | 0.931 | 0.931 | 0.931 | 0.931 | 0.932 | 0.932 | 0.932 | 0.932 | 0.933 | 0.934 | 0.935 |
| 178 | | – | – | 0.931 | 0.931 | 0.931 | 0.931 | 0.931 | 0.932 | 0.932 | 0.932 | 0.932 | 0.932 | 0.933 | 0.934 | 0.935 |
| 179 | | – | – | 0.931 | 0.931 | 0.931 | 0.931 | 0.931 | 0.932 | 0.932 | 0.932 | 0.932 | 0.933 | 0.933 | 0.934 | 0.935 |

Missing entries correspond to the points lying within the source. The length of the stainless-steel cable is 1 mm

## Results and Discussion

Table 2 compares the values of the dose-rate constants Λ of BEBIG sources to published values.[2,3,8] In the present study, this is 1.088 cGy/h/U (for both new and old designs). The GEANT4-based published values of Λ are 1.084 cGy/h/U and 1.087 cGy/h/U for the old and new source designs, respectively.[2,3] When $r_0$ = 1 cm, equation 9 represents the dose-rate constant for a point source, $\Lambda_p$. The calculated value of $\Lambda_p$ for a $^{60}$Co point source is 1.097 cGy/h/U, which is consistent with the value of 1.094 cGy/h/U reported by Papagiannis *et al.*[1] and the EDKnrc-based value of 1.107 ± 0.01 cGy/h/U reported by Selvam and Bhola.[8]

Table 3 compares the values of $g_L(r)$ for BEBIG $^{60}$C sources calculated in the present study and the EGSnrc-based published work.[8] At r = 2.5 mm, the EGSnrc-based published value[8] is higher by about 6% when compared with the value obtained in the present work. This is because the analytic calculation considers that there is charged particle equilibrium for all calculation points, including for regions close to the source. [Table 4] presents values of the anisotropy function for various radial distances from the source. The source cable length considered in this calculation was 1 mm for comparison with values published by Granero *et al.*[3] The analytically calculated data compares with the published data within 3%. [Tables 5 and 6] present the 2-D dose-rate distribution in water (in cGy/h/U) for the new source model with 5-mm and 1-mm-length stainless-steel cable, respectively. For the 1-mm cable length, the analytical data agree with the data published by Granero *et al.*[3] within 1%, and for the 5-mm cable length, the agreement is within

**Table 5: Dose rate distributions per unit air-kerma strength (cGy/h/U) around the new (model Co0.A86) BEBIG $^{60}$Co HDR source.**

| *Distance Along, z (cm)* | *Distance away, y (cm)* | | | | | | | | | | | | | | | |
|---|---|---|---|---|---|---|---|---|---|---|---|---|---|---|---|---|
| | *0* | *0.1* | *0.25* | *0.5* | *0.75* | *1* | *1.5* | *2* | *2.5* | *3* | *4* | *5* | *6* | *8* | *10* | *14* |
| −14 | 0.00372 | 0.00371 | 0.00371 | 0.00371 | 0.0037 | 0.00373 | 0.00391 | 0.00397 | 0.00406 | 0.00401 | 0.00389 | 0.00373 | 0.00353 | 0.0031 | 0.00265 | 0.00187 |
| −10 | 0.00795 | 0.00793 | 0.00793 | 0.00791 | 0.00804 | 0.00831 | 0.00851 | 0.00862 | 0.0085 | 0.00831 | 0.00781 | 0.00721 | 0.00658 | 0.00533 | 0.00425 | 0.00266 |
| −8 | 0.01291 | 0.01288 | 0.01287 | 0.01283 | 0.01341 | 0.01373 | 0.01387 | 0.01383 | 0.01345 | 0.01296 | 0.0118 | 0.01053 | 0.00929 | 0.00707 | 0.00535 | 0.00312 |
| −6 | 0.0238 | 0.0237 | 0.0237 | 0.0244 | 0.0253 | 0.0256 | 0.0255 | 0.0246 | 0.0233 | 0.0219 | 0.0188 | 0.0159 | 0.0133 | 0.0093 | 0.0066 | 0.0036 |
| −5 | 0.0348 | 0.0348 | 0.0347 | 0.0365 | 0.0374 | 0.0380 | 0.0367 | 0.0346 | 0.0321 | 0.0295 | 0.0243 | 0.0197 | 0.0159 | 0.01060 | 0.00728 | 0.00379 |
| −4 | 0.0550 | 0.0553 | 0.0551 | 0.0590 | 0.0597 | 0.0596 | 0.0560 | 0.0512 | 0.0460 | 0.0408 | 0.0316 | 0.0244 | 0.0189 | 0.01191 | 0.00792 | 0.00398 |
| −3 | 0.0979 | 0.0999 | 0.1028 | 0.1080 | 0.1078 | 0.1039 | 0.0928 | 0.0802 | 0.0682 | 0.0575 | 0.0409 | 0.0297 | 0.0221 | 0.01316 | 0.00849 | 0.00414 |
| −2.5 | 0.1416 | 0.1452 | 0.1525 | 0.1588 | 0.1536 | 0.1451 | 0.1241 | 0.1026 | 0.0838 | 0.0683 | 0.0462 | 0.0324 | 0.0236 | 0.01372 | 0.00873 | 0.00421 |
| −2 | 0.230 | 0.229 | 0.245 | 0.248 | 0.233 | 0.213 | 0.170 | 0.132 | 0.1029 | 0.0806 | 0.0517 | 0.0351 | 0.0250 | 0.01422 | 0.00894 | 0.00426 |
| −1.5 | 0.414 | 0.412 | 0.447 | 0.429 | 0.383 | 0.332 | 0.238 | 0.171 | 0.1247 | 0.0935 | 0.0568 | 0.0375 | 0.0263 | 0.01462 | 0.00911 | 0.00431 |
| −1 | 0.956 | 1.001 | 1.027 | 0.879 | 0.700 | 0.544 | 0.332 | 0.214 | 0.1467 | 0.1056 | 0.0612 | 0.0394 | 0.0272 | 0.01493 | 0.00924 | 0.00434 |
| −0.5 | … | 4.59 | 3.74 | 2.23 | 1.349 | 0.871 | 0.432 | 0.253 | 0.1640 | 0.1144 | 0.0641 | 0.0406 | 0.0278 | 0.01512 | 0.00931 | 0.00436 |
| −0.25 | … | 21.66 | 9.40 | 3.49 | 1.737 | 1.021 | 0.467 | 0.264 | 0.1689 | 0.1168 | 0.0649 | 0.0409 | 0.0279 | 0.01516 | 0.00933 | 0.00436 |
| -0.15 | … | 47.65 | 12.80 | 3.94 | 1.849 | 1.060 | 0.475 | 0.267 | 0.1700 | 0.1173 | 0.0650 | 0.0410 | 0.0280 | 0.01517 | 0.00934 | 0.00436 |
| -0.1 | … | 58.83 | 14.20 | 4.10 | 1.886 | 1.072 | 0.478 | 0.268 | 0.1704 | 0.1175 | 0.0651 | 0.0410 | 0.0280 | 0.01518 | 0.00934 | 0.00436 |
| 0 | … | 58.84 | 15.44 | 4.24 | 1.92 | 1.072 | 0.480 | 0.268 | 0.1706 | 0.1176 | 0.0651 | 0.0412 | 0.0280 | 0.01518 | 0.00934 | 0.00436 |
| 0.1 | … | 58.83 | 14.20 | 4.10 | 1.886 | 1.072 | 0.478 | 0.268 | 0.1704 | 0.1175 | 0.0651 | 0.0410 | 0.0280 | 0.01518 | 0.00934 | 0.00436 |
| 0.15 | … | 47.65 | 12.80 | 3.94 | 1.849 | 1.060 | 0.475 | 0.267 | 0.1700 | 0.1173 | 0.0650 | 0.0410 | 0.0280 | 0.01517 | 0.00934 | 0.00436 |
| 0.25 | … | 21.66 | 9.40 | 3.49 | 1.737 | 1.021 | 0.467 | 0.264 | 0.1689 | 0.1168 | 0.0649 | 0.0409 | 0.0279 | 0.01516 | 0.00933 | 0.00436 |
| 0.5 | 4.79 | 4.59 | 3.74 | 2.23 | 1.349 | 0.871 | 0.432 | 0.253 | 0.1640 | 0.1144 | 0.0641 | 0.0406 | 0.0278 | 0.01512 | 0.00931 | 0.00436 |
| 0.75 | 1.967 | 1.924 | 1.796 | 1.368 | 0.976 | 0.697 | 0.384 | 0.235 | 0.1563 | 0.1105 | 0.0628 | 0.0401 | 0.0275 | 0.01504 | 0.00928 | 0.00435 |
| 1 | 1.075 | 1.062 | 1.027 | 0.879 | 0.700 | 0.544 | 0.332 | 0.214 | 0.1467 | 0.1056 | 0.0612 | 0.0394 | 0.0272 | 0.01493 | 0.00924 | 0.00434 |
| 1.5 | 0.466 | 0.463 | 0.459 | 0.429 | 0.383 | 0.332 | 0.238 | 0.171 | 0.1247 | 0.0935 | 0.0568 | 0.0375 | 0.0263 | 0.01462 | 0.00911 | 0.00431 |
| 2 | 0.259 | 0.257 | 0.254 | 0.248 | 0.233 | 0.213 | 0.170 | 0.132 | 0.1029 | 0.0806 | 0.0517 | 0.0351 | 0.0250 | 0.01422 | 0.00894 | 0.00426 |
| 2.5 | 0.1637 | 0.1632 | 0.1618 | 0.1588 | 0.1536 | 0.1451 | 0.1241 | 0.1026 | 0.0838 | 0.0683 | 0.0462 | 0.0324 | 0.0236 | 0.01372 | 0.00873 | 0.00421 |
| 3 | 0.1126 | 0.1123 | 0.1116 | 0.1109 | 0.1078 | 0.1039 | 0.0928 | 0.0802 | 0.0682 | 0.0575 | 0.0409 | 0.0297 | 0.0221 | 0.01316 | 0.00849 | 0.00414 |
| 4 | 0.0623 | 0.0621 | 0.0619 | 0.0611 | 0.0607 | 0.0596 | 0.0560 | 0.0512 | 0.0460 | 0.0408 | 0.0316 | 0.0244 | 0.0189 | 0.01191 | 0.00792 | 0.00398 |
| 5 | 0.0392 | 0.0391 | 0.0390 | 0.0387 | 0.0388 | 0.0380 | 0.0367 | 0.0346 | 0.0321 | 0.0295 | 0.0243 | 0.0197 | 0.0159 | 0.01060 | 0.00728 | 0.00379 |
| 6 | 0.0267 | 0.0267 | 0.0266 | 0.0265 | 0.0262 | 0.0263 | 0.0255 | 0.0246 | 0.0233 | 0.0219 | 0.0188 | 0.0159 | 0.0133 | 0.00932 | 0.00662 | 0.00358 |
| 8 | 0.01449 | 0.01446 | 0.01445 | 0.0144 | 0.01433 | 0.01422 | 0.01411 | 0.01383 | 0.01345 | 0.01296 | 0.0118 | 0.01053 | 0.00929 | 0.00707 | 0.00535 | 0.00312 |
| 10 | 0.00892 | 0.0089 | 0.0089 | 0.00888 | 0.00885 | 0.0088 | 0.00883 | 0.00862 | 0.0085 | 0.00831 | 0.00781 | 0.00721 | 0.00658 | 0.00533 | 0.00425 | 0.00266 |
| 14 | 0.00417 | 0.00416 | 0.00416 | 0.00415 | 0.00415 | 0.00414 | 0.0041 | 0.00413 | 0.00398 | 0.00401 | 0.00389 | 0.00373 | 0.00353 | 0.0031 | 0.00265 | 0.00187 |

The coordinate axes are defined in Figure 1. The source is along the z-axis, with positive z toward the source tip. The length of the stainless-steel cable is 5 mm

**Table 6: Dose rate distributions per unit air-kerma strength (cGy/h/U) around the new (model Co0.A86) BEBIG $^{60}$Co HDR source.**

| *Distance along, z (cm)* | *Distance away, y (cm)* | | | | | | | | | | | | | | |
|---|---|---|---|---|---|---|---|---|---|---|---|---|---|---|---|
| | *0* | *0.25* | *0.5* | *0.75* | *1* | *1.5* | *2* | *2.5* | *3* | *4* | *5* | *6* | *8* | *10* | *14* |
| −14 | 0.00411 | 0.00407 | 0.00407 | 0.00406 | 0.00405 | 0.00402 | 0.00405 | 0.00404 | 0.00401 | 0.00389 | 0.00373 | 0.00353 | 0.00310 | 0.00265 | 0.00187 |
| −10 | 0.00877 | 0.00871 | 0.00869 | 0.00866 | 0.00861 | 0.00867 | 0.00863 | 0.00850 | 0.00831 | 0.00781 | 0.00721 | 0.00658 | 0.00533 | 0.00425 | 0.00266 |
| −8 | 0.01424 | 0.01414 | 0.01410 | 0.01402 | 0.01391 | 0.01407 | 0.01384 | 0.01345 | 0.01296 | 0.01180 | 0.01054 | 0.00929 | 0.00707 | 0.00535 | 0.00312 |
| −6 | 0.0263 | 0.0261 | 0.0259 | 0.0257 | 0.0260 | 0.0256 | 0.0246 | 0.0233 | 0.0219 | 0.01883 | 0.01591 | 0.01332 | 0.00932 | 0.00662 | 0.00358 |
| −5 | 0.0385 | 0.0382 | 0.0378 | 0.0381 | 0.0380 | 0.0367 | 0.0346 | 0.0322 | 0.0295 | 0.0243 | 0.0197 | 0.01594 | 0.01060 | 0.00728 | 0.00379 |
| −4 | 0.0611 | 0.0606 | 0.0598 | 0.0606 | 0.0596 | 0.0560 | 0.0512 | 0.0460 | 0.0408 | 0.0316 | 0.0244 | 0.01893 | 0.01191 | 0.00792 | 0.00398 |
| −3 | 0.1106 | 0.1092 | 0.1098 | 0.1079 | 0.1040 | 0.0928 | 0.0803 | 0.0682 | 0.0575 | 0.0409 | 0.0297 | 0.0221 | 0.01316 | 0.00849 | 0.00414 |
| −2.5 | 0.1607 | 0.1583 | 0.1590 | 0.1537 | 0.1452 | 0.1241 | 0.1027 | 0.0838 | 0.0683 | 0.0462 | 0.0324 | 0.0236 | 0.01372 | 0.00873 | 0.00421 |
| −2 | 0.254 | 0.248 | 0.248 | 0.233 | 0.213 | 0.1703 | 0.1325 | 0.1029 | 0.0806 | 0.0517 | 0.0351 | 0.0250 | 0.01422 | 0.00894 | 0.00426 |
| −1.5 | 0.457 | 0.454 | 0.430 | 0.384 | 0.332 | 0.2385 | 0.1707 | 0.1247 | 0.0936 | 0.0568 | 0.0375 | 0.0263 | 0.01462 | 0.00911 | 0.00431 |
| −1 | 1.055 | 1.028 | 0.879 | 0.700 | 0.544 | 0.332 | 0.214 | 0.1467 | 0.1056 | 0.0612 | 0.0394 | 0.0272 | 0.01493 | 0.00924 | 0.00434 |
| -0.75 | | 1.797 | 1.368 | 0.976 | 0.698 | 0.384 | 0.235 | 0.1563 | 0.1105 | 0.0628 | 0.0401 | 0.0275 | 0.01504 | 0.00928 | 0.00435 |
| −0.5 | … | 3.75 | 2.23 | 1.349 | 0.871 | 0.432 | 0.253 | 0.1640 | 0.1144 | 0.0641 | 0.0406 | 0.0278 | 0.01512 | 0.00931 | 0.00436 |
| −0.25 | … | 9.40 | 3.49 | 1.737 | 1.021 | 0.467 | 0.264 | 0.1689 | 0.1168 | 0.0649 | 0.0409 | 0.0279 | 0.01516 | 0.00933 | 0.00436 |
| 0 | … | 15.44 | 4.24 | 1.917 | 1.083 | 0.480 | 0.268 | 0.1706 | 0.1176 | 0.0651 | 0.0410 | 0.0280 | 0.01518 | 0.00934 | 0.00436 |
| 0.25 | … | 9.40 | 3.49 | 1.737 | 1.021 | 0.467 | 0.264 | 0.1689 | 0.1168 | 0.0649 | 0.0409 | 0.0279 | 0.01516 | 0.00933 | 0.00436 |
| 0.5 | 4.78 | 3.77 | 2.23 | 1.349 | 0.871 | 0.432 | 0.253 | 0.1640 | 0.1144 | 0.0641 | 0.0406 | 0.0278 | 0.01512 | 0.00931 | 0.00436 |
| 0.75 | 1.96 | 1.797 | 1.368 | 0.976 | 0.698 | 0.384 | 0.235 | 0.1563 | 0.1105 | 0.0628 | 0.0401 | 0.0275 | 0.01504 | 0.00928 | 0.00435 |
| 1 | 1.074 | 1.028 | 0.879 | 0.700 | 0.544 | 0.332 | 0.214 | 0.1467 | 0.1056 | 0.0612 | 0.0394 | 0.0272 | 0.01493 | 0.00924 | 0.00434 |
| 1.5 | 0.465 | 0.459 | 0.430 | 0.384 | 0.332 | 0.2385 | 0.1707 | 0.1247 | 0.0936 | 0.0568 | 0.0375 | 0.0263 | 0.01462 | 0.00911 | 0.00431 |
| 2 | 0.258 | 0.254 | 0.248 | 0.233 | 0.213 | 0.1703 | 0.1325 | 0.1029 | 0.0806 | 0.0517 | 0.0351 | 0.0250 | 0.01422 | 0.00894 | 0.00426 |
| 2.5 | 0.1635 | 0.1620 | 0.1590 | 0.1537 | 0.1452 | 0.1241 | 0.1027 | 0.0838 | 0.0683 | 0.0462 | 0.0324 | 0.0236 | 0.01372 | 0.00873 | 0.00421 |
| 3 | 0.1125 | 0.1118 | 0.1111 | 0.1079 | 0.1040 | 0.0928 | 0.0803 | 0.0682 | 0.0575 | 0.0409 | 0.0297 | 0.0221 | 0.01316 | 0.00849 | 0.00414 |
| 4 | 0.0622 | 0.0620 | 0.0612 | 0.0608 | 0.0596 | 0.0560 | 0.0512 | 0.0460 | 0.0408 | 0.0316 | 0.0244 | 0.01893 | 0.01191 | 0.00792 | 0.00398 |
| 5 | 0.0391 | 0.0391 | 0.0387 | 0.0389 | 0.0380 | 0.0367 | 0.0346 | 0.0322 | 0.0295 | 0.0243 | 0.0197 | 0.01594 | 0.01060 | 0.00728 | 0.00379 |
| 6 | 0.0267 | 0.0267 | 0.0265 | 0.0263 | 0.0263 | 0.0256 | 0.0246 | 0.0233 | 0.0219 | 0.01883 | 0.01591 | 0.01332 | 0.00932 | 0.00662 | 0.00358 |
| 8 | 0.01447 | 0.01447 | 0.01443 | 0.01435 | 0.01424 | 0.01413 | 0.01384 | 0.01345 | 0.01296 | 0.01180 | 0.01054 | 0.00929 | 0.00707 | 0.00535 | 0.00312 |
| 10 | 0.00890 | 0.00891 | 0.00889 | 0.00886 | 0.00882 | 0.00884 | 0.00863 | 0.00850 | 0.00831 | 0.00781 | 0.00721 | 0.00658 | 0.00533 | 0.00425 | 0.00266 |
| 14 | 0.00416 | 0.00417 | 0.00416 | 0.00415 | 0.00414 | 0.00411 | 0.00414 | 0.00407 | 0.00401 | 0.00389 | 0.00373 | 0.00353 | 0.00310 | 0.00265 | 0.00187 |

The coordinate axes are defined in Figure 1. The source is along the z-axis, with positive z toward the source tip. The length of the stainless-steel cable is 1 mm

3%. For regions where charged-particle equilibrium exists, a comparison of these data with the corresponding EGSnrc-based published data[8] suggests that the analytically calculated values are comparable to within 0.5% for most points, and the maximum deviation is about 3%.

## Conclusions

We have proposed a point-source-based simple analytic method for calculating the dose-rate distribution in water in units of cGy/h/U for a BEBIG $^{60}$Co HDR source. Using this method, we calculated TG-43 parameters such as the dose-rate constant, radial dose function and anisotropy function. We also calculated a 2-D dose-rate table in Cartesian format. The proposed analytic method needed best-fit parameters for linear attenuation coefficients of source and filtration materials for regions close to the source axis. The analytic model proposed is easy to implement in radiotherapy treatment-planning dose calculations. For regions where electronic equilibrium exists, a comparison between the analytically calculated and published Monte Carlo-based data shows good agreement (for most calculation points, agreement was within 0.5%, and the maximum deviation was about 3%). The dose-rate data calculated with this method could be used for verifying the results of RTPS or directly as input data for radiotherapy treatment-planning dose calculations.

## Acknowledgment

The authors wish to thank Dr. Y. S. Mayya, Head, Radiological Physics and Advisory Division, Bhabha Atomic Research Centre (BARC), and Dr. G. Chourasiya, BARC, for their encouragement and support throughout this project.

## References

1. Papagiannis P, Angelopoulos A, Pantelis E, Sakelliou L, Karaiskos P, Shimizu Y. Monte Carlo dosimerty of $^{60}$Co HDR brachytherapy sources. Med. Phys.2003;30:712-21.
2. Ballester F, Granero D, Perez-Calatayud J, Casal E, Agramunt S, Cases R. Monte Carlo dosimetric study of the BEBIG Co-60 HDR source. Phys Med Biol 2005;50:309-16.
3. Granero D, Perez-Calatayud J, Ballester F. Technical note: Dosimertic study of a new Co-60 source used in brachytherapy. Med Phys 2007;34:3485-8.
4. Richter J, Baier K, Flentje M. Comparison of $^{60}$Co and $^{192}$Ir sources in High Dose Rate Afterloading Brachytherapy. Strahlenther Onkol 2008;184:187-92.
5. Nath R, Anderson L, Luxton G, Weaver A, Williamson F, Meigooni S. Dosimetry of interstitial brachytherapy sources: Recommendations of the AAPM Radiation Therapy Committee Task Group 43. Med Phys 1995;22:209-34.
6. Rivard J, Coursey M, Dewerd A, Hanson F, Huq S, Ibbott S, *et al*. Update of AAPM task Group No. 43 Report: A revised AAPM protocol for brachytherapy dose calculations. Med Phys 2004;31:633-74.
7. Nath R, Anderson L, Meli A, Olch J, Stitt A, Williamson F. Code of practice for brachytherapy physics: Report of the AAPM Radiation Therapy Committee Task Group No. 56. Med. Phys 1997;24:1557-98.
8. Selvam P, Bhola S. Technical Note: EGSnrc-based dosimetric study of the BEBIG $^{60}$Co HDR Brachytherapy sources. Med Phy 2010;37:1365-70.
9. Sievert M. Die Intensitatsverteilung der primären gamma-Strahlung in der Na¨he medizinischer Radiumpräparate. Acta Radiol 1921;1:89-128.
10. Williamson F. Monte Carlo and Analytic calculation of absorbed dose near $^{137}$Cs intracavitary sources. Int J Radiat Oncol BiolPhys 1988;15:227-37.
11. Williamson F. The Sievert integral revisited: Evaluation and extension to $^{125}$1, $^{169}$Yb, and $^{192}$1r brachytherapy sources. Int J Radiat Oncol Biol Phys 1996;36:1239-50.
12. Lizhong L, Prasad C, Bassano A. Determination of $^{137}$Cs dosimetry parameters according to AAPM TG--43 formalism. Med Phys 2004;31:477-83.
13. Ballester F, Lluch L, Limami Y, Serrano A, Perez-Calatayud J, Lliso A. A Monte Carlo investigation of the dosimetric characteristics of the CSM11 $^{137}$Cs source from CIS. Med Phys 2000;27:2182-9.
14. Casal E, Ballester F, Lluch L, Perez-Calatayud J, Lliso F. Monte Carlo Calculations of dose rate distributions around the Amersham CDCS-M-type $^{137}$Cs source. Med Phys 2000;27:132-40.
15. Perez-Calatayud J, Ballester F, Serrano-Andres A, Lluch L, Puchades V, Limami Y, *et al*. Dosimetric characteristics of the CDC-type miniature cylindrical $^{137}$Cs brachytherapy sources. Med Phys 2002;29:538-43.
16. Perez-Calatayud J, Lliso F, Carmona V, Ballester F, Hernandez C. Monte Carlo calculations of dose rate distributions around 0.5 and 0.6 mm in diameter $^{192}$Ir wires. Med Phys 1999;26:395-401.
17. Pantelis E, Baltas D, Dardoufas K, Karaiskos P, Papagiannis P, Rosaki H, *et al*. On the dosimertic accuracy of a Sievert Integration model in the proximity of $^{192}$Ir HDR sources. Int J Radiat Oncol Biol Phys 2002;53:1071-84.
18. Karaiskos P, Sakelliou L, Sandilos P. Limitations of the point and line source approximations for the determination of the Geometry factor around brachytherapy sources. Med Phys 2000;27:124-8.
19. Berger J. Energy deposition in water by photons from point isotropic sources. J Nucl Med Suppl 1968;1:17-25.
20. Hubbel H, Seltzer M. Tables of X-ray mass attenuation coefficients and mass energy absorption coefficient 1 keV to 20 MeV for elements Z=1 to 92 and 48 additional substances of dosimetric interest. *NISTIR* 5632: Gaithersburg, MD: NIST; 1995.
21. Kartha P, Kenney N, Cameron R. An experimental determination of the absorption and buildup factor in water for radium, cobalt 60, and cesium 137 gamma rays. Am J RoenTG-enol 1996;96:66-9.
22. Meisberger L, Keller J, Shalek J. Effective Attenuation in Water of the Gamma Rays of Gold 198, Iridium 192, Cesium 137, Radium 226, and Cobalt 60. Radiol 1968;93:953-7.
23. Van Kleffens J, Star M. Application of Stereo X-Ray Photogrammetry (SRM) in the Determination of Absorbed Dose Values during Intracavitary Radiation Therapy. Int J Radiat Oncol Biol Phys 1979;5:559.
24. Kornelnen R, Young E. Brachythcrapy buildup factors. Br Rodiol 1981;54:136.
25. Angelopoulost A, Perris A, Sakellarioug K, Sakelliouii L, Sarigiannist K, Zarrist G. Accurate Monte Carlo calculations of the combined attenuation and build up factors, for energies (20-1500 keV) and distances (0-10 cm) relevant in brachytherapy. Phys Med Biol 1991;36:763-78.
26. Papagiannis P, Angelopoulos A, Pantelis E, Sakelliou L, Baltas D, Karaiskos P, *et al*. Dosimetry Comparison of $^{192}$Ir sources. Med.Phys 2002;29:2239-46.
27. Rivard J. Refinements to the geometry factor used in the AAPM Task Group Report No. 43 necessary for brachytherapy dosimetry calculations. Med Phys 1999;26:2445-50.
28. Cassell J. A fundamental approach to the design of a dose rate calculation for use in brachytherapy planning. Br J Radiol 1983;56:113-9.

**How to cite this article:** Bhola S, Selvam TP, Sridhar S, Vishwakarma RS. An analytic approach to the dosimetry of a new BEBIG 60 Co high-dose-rate brachytherapy source. J Med Phys 2012;37:129-37.
**Source of Support:** Nil, **Conflict of Interest:** None declared.